

To appear in the Astrophysical Journal: Version 2006 Nov 30

Detection of ^{13}C Isotopomers of Molecule HC_7N

G. Langston¹

National Radio Astronomy Observatory, P.O. Box 2, Green Bank, WV 24944

glangsto@nrao.edu

and

B. Turner²

National Radio Astronomy Observatory, 520 Edgemont Rd, Charlottesville, VA 22901

bturner@nrao.edu

ABSTRACT

The ^{13}C substitutions of molecule HC_7N were observed in TMC-1 using the $J = 12 - 11$, $J = 13 - 12$ rotational transitions in the frequency range 12.4 to 13.6 GHz. We present the first detection the ^{13}C isotopic species of HC_7N in the interstellar medium, based on the average of a number of weak rotational transitions.

This paper describes the calibration and data averaging process that is also used in a search for large cyanopolyynes in TMC-1 using the 100m Robert C. Byrd Green Bank Telescope (GBT). The capabilities of the GBT 11 to 15 GHz observing system are described along with a discussion of numerical methods for averaging observations of a number of weak spectral lines to detect new interstellar molecules.

Subject headings: astrochemistry, ISM:molecules, HC_7N , Taurus Molecular Cloud, TMC

1. Introduction

The large cyanopolyynes molecules, HC_5N , HC_7N , and HC_9N , are seen in great abundance towards the Taurus Molecular Cloud 1 (TMC-1) over a very wide frequency range (e.g.

Olano, Walmsley and Wilson (1988), Bell et al (1997), Kaifu et al. (2004), Kalenskii et al. (2004)). The detection of these cyanopolyynes demonstrates that large organic molecules are forming in interstellar (IS) medium.

A notable property of the cyanopolyynes is the relatively high intensity rotational transition lines seen towards astronomical sources. The strong line intensity is due to the simplicity of the radio spectra of these linear carbon chains with large dipole moments. The cyanopolyynes are valuable guides for the study of all large molecule chemistry in the IS medium. The chemical relationships and distribution in TMC-1 of molecules HC_3N , HC_5N , HC_7N , and HC_9N have been studied by many authors, including Pratap et al. (1997), Dickens et al (2001) and Turner et al (2005). The relative abundance of deuterated and ^{13}C isotopomers of molecules in the IS medium is an important test for models of IS chemistry (Turner 2001).

In § 2 we present the observations and the technique for calibration and averaging of the data. In § 3 we combine multiple observations of different rotational transitions of a single molecule. In § 4 we compare our measurements with earlier observations. In § 5 the results are summarized.

2. Observations

We present selected observations of TMC-1 which are part of a search for large cyanopolyynes ($HC_{11}N$ and $HC_{13}N$) in the interstellar medium. The large cyanopolyne search is reported by Langston et al. (2007). The data presented here are from daily system check observations to confirm proper operation of the antenna pointing, receiver sensitivity and spectrometer configuration. All the search observations were made in the period January 14, 2006 to September 10, 2006. The observations were made using the NRAO ¹ Robert C. Byrd Green Bank Telescope (GBT). We present observations of TMC-GB (R.A. $4^h41^m42.05^s$, δ $25^\circ41'27.5''$ J2000), and TMC- HC_9N (R.A. $4^h41^m44.7^s$, δ $25^\circ40'56''$ J2000). Figure 1, from Langston and Turner (2007), shows a map of the HC_9N emission with the locations of TMC- HC_9N and TMC-GB marked.

For these observations, the GBT was configured using the Astronomers Integrated Desktop, ASTRID, for use of the Ku-band (11.7 to 15.6 GHz) dual beam receiver. At 11.7 GHz the FWHM beam width is $65''$ and at 15 GHz the FWHM beam width is $50.8''$. The GBT

¹The National Radio Astronomy Observatory (NRAO) is a facility of the National Science Foundation operated under cooperative agreement by Associated Universities, Inc.

Ku-band receiver has two feeds, separated by an angular offset of $330''$ in cross-elevation direction on the sky.

Before each spectral line observing session, we first performed PEAK and FOCUS observations on bright continuum radio source 3C123. Unless the weather was very poor, the first PEAK and FOCUS observations were almost always successful. Typical pointing offsets were under $10''$ in either axis. In the case of unusually large offsets ($d\theta > 20''$), found only during poor weather, the PEAK observations were repeated.

All spectral line observations were performed using the ASTRID NOD procedure. The NOD procedure allows simultaneous "signal" and "reference" observations using both beams of the Ku-band receiver. A NOD observation consists of two 4-minute scans, one with the first beam of the dual beam receiver pointing towards the target location, followed by a second scan with the second beam pointed towards the target location. The Ku-band receiver is oriented so that the two beams observe the same target elevation. During the spectral line observations, the GBT spectrometer is configured to simultaneously collect spectra at the same frequencies in both beams. For these observations, the spectrometer continuously controlled injection of a 2-3 K noise diode signal into both beams via RF inputs of both polarizations. The noise diode was turned on and off at a 1 Hz rate.

For the $HC_{13}N$ search observations, the GBT IF path and spectrometer were configured to simultaneously collect four 50 MHz wide spectral bands centered on four different frequencies. The integration time was 30 seconds and the scan duration was 4 minutes, yielding 8 spectra for each of the two polarizations of the dual beams. The noise diode ON and noise diode OFF spectra were separately recorded. During a four minute scan, a total of $8(\text{integrations}) \times 2(\text{beams}) \times 2(\text{polarizations}) \times 2(\text{noise diode states}) = 64$ spectra were recorded. The GBT spectrometer has 3 level and 9 level sampling modes. The 3 level sampling mode was used, yielding a channel spacing $\Delta\nu = 3.05176$ kHz. At 13 GHz this spectral resolution corresponds to 0.07 km/sec channels.

To confirm proper operations of the GBT spectrometer, at the beginning of most sessions we performed test NOD observations on TMC-GB, simultaneously observed four strong cyanopolyne rotational transition lines, HC_5N $J = 5 - 4$, HC_7N $J = 12 - 11$, HC_7N $J = 11 - 10$ and HC_9N $J = 23 - 22$, at frequencies listed in table 1. In the short (4 minute) pair of NOD observations, all four lines are visible at high signal to noise ratio.

In the course of the large cyanopolyne search, a map of TMC-1 was made in the HC_9N lines with 1 arc-minute angular resolution. The intensity versus position maps are described in Langston and Turner (2007). The HC_9N peak emission is 16 % stronger than at the TMC-GB location. This TMC- HC_9N position was observed to confirm the detection

isotopomers of HC_7N at TMC-GB. This position was observed for a total of 4 hours on September 6 and 2 hours on September 7, 2006. The GBT spectrometer was configured for high resolution, 12.5 MHz 3 level samplers, four spectral band, dual polarization observation.

For the 3 level 12.5 MHz bandwidth spectrometer configuration, the channel spacing is 4 times smaller than the 50 MHz configuration, $\Delta\nu = 0.76294$ kHz. At 13 GHz this spectral resolution corresponds to 0.018 km/sec channels.

For the 12.5 MHz spectrometer mode, two different IF input configurations were required for observation of all seven ^{13}C isotopomers of HC_7N for the $J = 12-11$ rotation transitions, plus the HC_7N , DC_7N and $HC_7^{15}N$ transitions.

2.1. T_A Calibration

The raw data were calibrated to an antenna temperature scale by the $T_{sys,reference} \times (C_{signal}(\nu) - C_{reference}(\nu))/C_{reference}(\nu)$ technique, where $C_{signal}(\nu)$ is the measured intensity (raw counts) as a function of frequency, ν , when observing the source location, and $C_{reference}(\nu)$ is the measured intensity (raw counts) when observing one of the two reference locations. The system temperature was computed for each spectral channel of each reference location. The system temperature for each channel was defined as average of the noise diode ON and noise diode OFF spectra divided by the difference of noise diode ON and noise diode OFF spectra, then multiplied by the effective temperature of the calibration noise diode value measured in the laboratory. For the purposes of intensity calibration, the reference system temperature, $T_{sys,reference}$ is defined as the median of the calculated system temperatures for the central 40 MHz of the 50 MHz spectral band. This procedure was repeated for each of the four spectral bands. For the 12.5 MHz bandwidth observations the central 10 MHz of each spectral bands was used for T_{sys} calibration.

The two Ku-band beams are separated on the sky by an amount smaller than the maximum size of TMC-1. To compensate for line contamination of the source spectrum due to possible emission in the reference spectra, the calibration was performed using a median filtered reference spectrum. The median reference spectrum is a smoothed version of the observed reference spectrum. The median spectrum is the median of all channels of the reference spectrum within a 0.5 MHz bandwidth centered on the frequency of the input channel. The filter width is wider than the 0.021 MHz FWHM TMC-1 line width.

Figure 2 shows uncalibrated intensity versus frequency spectra, the signal beam spectrum (top), the reference beam spectrum (bottom). The frequency axis is set assuming a LSR source velocity of 5.815 ± 0.010 km/sec. The 0.5 MHz wide median filtered (smooth)

signal and reference spectra are overlaid on the observed spectra. The high effectiveness of median filtering in removing spectral lines is shown for the median of the signal spectrum in figure 2.

The median width must be narrow enough to preserve significant variations in the IF gain as a function of frequency, but must be wide enough to reduce the noise in the reference spectrum and to reject any weak narrow lines at the reference position. Calibration using the median spectrum produces a higher signal to noise ratio spectrum than calibration without smoothing the reference spectrum.

2.2. T_B Calibration

The T_A scaled data were further calibrated to brightness temperature (corrected for atmospheric opacity) in order to compare these results with previous observations and computing the physical properties of TMC-1. The T_B calibration was performed assuming TMC-1 is more extended than the GBT primary beam in the frequency range 11.6 to 14.5 GHz. This assumption is confirmed by our HC_9N mapping observations.

The GBT beam efficiency was computed assuming

$$\eta_A(\nu) = 0.71 \exp\left[-\left(\frac{\nu}{61.3 \text{ GHz}}\right)^2\right] \quad (1)$$

and

$$\eta_B(\nu) = 1.37 \eta_A(\nu) \quad (2)$$

where ν is the frequency in GHz. Equation 1 is the Ruze equation (Ruze 1966) assuming the GBT surface accuracy is 390 microns RMS ² and $\eta_A(\nu = 0) = 0.71$.

For each observing epoch, the average atmospheric opacity, τ , at 13.0 GHz was adopted for all all observed frequency bands. The adopted τ values ranged from 0.01 to 0.04, with a median value of ~ 0.019 . The τ values were computed based on a model for the local weather (R. Madallena 2006 ³), using measured weather data at nearby locations.

Figure 3 shows the T_B calibrated average spectrum of the HC_5N $J = 5 - 4$ line. The upper (black) spectrum shows the average of right and left circular polarization using the GBT beam efficiency model of equation 2 and corrected for atmospheric opacity. The two lower spectra are right (red) and left (blue) circular polarizations, each T_A calibrated. The

²<http://wwwlocal.gb.nrao.edu/gbtprops/man/GBTpg/>

³<http://www.gb.nrao.edu/~rmaddale/Weather/>

GBT efficiency factor, η_B , is 0.926 at 13535 MHz. For the median opacity, $\tau = 0.019$, the opacity correction factor is small, 1.02.

A spectral baseline is computed for each polarization separately. The spectral baseline is the median of the observed spectrum computed over a 0.5 MHz width centered on each channel of the spectrum. A median baseline is commonly used for GBT spectral line observations, which cover a relatively wide bandwidth (e.g. Hollis et al. 2004). The near identical intensity of the left and right circular polarization shows the good agreement of the two independent calibrations of the intensity of the two polarizations. The HC_5N $J = 5 - 4$ line was chosen as the calibration example to illustrate the importance of using a wide median filter window for baseline subtraction, to preserve the line intensity in the case of a number of closely spaced transitions. The HC_5N hyperfine transitions are sufficiently close that a narrower median filter width in the baseline calculation would reduce line intensity.

The other 3 rotational transitions observed each epoch are similarly calibrated. Figure 4 shows T_B intensity versus frequency plot for the four 50 MHz bands observed with the GBT spectrometer, when configured for the four frequency band and dual polarization test mode. Figure 5 shows the T_B calibrated spectra for all four lines in an intensity versus velocity plot.

2.3. Frequency Smearing due to Doppler tracking

The GBT local oscillator (LO) and intermediate frequency (IF) system is designed with one doppler tracking system. This has important consequences for observations using the GBT spectrometer in the four frequency band mode. The GBT system is designed to accurately track the reference frame for the center frequency of the first of the four bands. All other up and down frequency conversions are done in topocentric frame. The consequence of this design is that the observations for the first frequency band may be averaged for long durations, without frequency smearing of the molecular lines. For the remaining three frequency bands, care must be taken to properly align the spectra before averaging over several epochs. We have written a number of *Interactive Display Language* (IDL) ⁴ scripts to properly account for the shift in center frequency of the spectral bands over time. The data were reduced using GBTIDL ⁵ and `rt_idl` ⁶, data reduction packages. During the observations,

⁴Research Systems, Inc. <http://www.rsinc.com/idl>

⁵ Developed by the National Radio Astronomy Observatory, documentation at <http://gbtidl.sourceforge.net/>

⁶Documentation on `rt_idl` is available on the web at http://www.gb.nrao.edu/~glangsto/rt_idl

the data were examined using `rt_id1` a set of display scripts created by G.L. for real-time display. A goal of the present work is to demonstrate the effectiveness of these procedures.

Our process of averaging spectra with different channel bandwidths and center frequencies is similar to the standard process for convolving irregularly sampled continuum intensity values onto an image grid (Dickey 2002). The process of combining the spectra, $S_e(\nu)$, from each epoch of observation has three major components. Before averaging, each of the $S_e(\nu)$ spectra are T_B calibrated.

Convolving function The first step in computing an average spectrum from a set of spectra from each epoch, $S_e(\nu)$, with different center frequencies and channel separation is definition of the output spectral sum, $Sum(\nu)$, and the convolving function $W(\nu)$. For spectral gridding, convolution function, $W(\nu - \nu_0)$, is defined in equation 3 as a Gaussian function with FWHM width equal to half the channel width of the first input spectrum, $\Delta\nu_0$ (for this application, all spectra had nearly identical channel spacings). The offset between the input frequency channel of a single observation and the frequency of a channel of the average spectra is $\Delta\nu = \nu - \nu_0$.

$$W(\Delta\nu) = \exp[-4 \ln(2)(\Delta\nu/\Delta\nu_0)^2] \quad (3)$$

This convolving function definition has three desired properties. The first is at zero frequency offset the convolving function is unity, i.e. $W(\Delta\nu = 0) = 1$. The second property is if the offset is half the channel width, then the two adjacent channels are averaged, i.e. $W(\Delta\nu = \pm\Delta\nu_0/2) = 0.5$. The third property is if the input channels have a large frequency offset, then these channels make little contribution to the average, i.e. $W(\Delta\nu = \pm 3\Delta\nu_0) \sim 1.5 \times 10^{-11}$. For our application, the weighting function kernel width is ± 5 channels.

Convolution The spectra from each epoch is gridded into the output spectrum in the same manner. For each channel in the output spectrum (frequency ν), the closest channels in the input spectrum were found (frequency ν_i). Next over the convolution function kernel size, the frequency offset between the input spectrum and the output channel was computed. The convolution function was computed and multiplied by a constant spectral weight for each epoch of observation. The spectrum weight is $W_e = t_{int}/T_{sys}^2$, where t_{int} is the integration time and T_{sys} is the system temperature. This weighting yields the optimum signal to noise ratio in the output spectrum. The input spectrum was multiplied by the weighted convolution kernel and summed into the output spectrum. The weighted convolution kernel is summed into the convolution weight spectrum.

$$Sum(\nu) = \sum_{epochs} \sum_{i=-5}^{+5} W_e W(\nu - \nu_i) S_e(\nu_i) \quad (4)$$

$$Weight(\nu) = \sum_{epochs} \sum_{i=-5}^{+5} W_e W(\nu - \nu_i) \quad (5)$$

Normalization

The output spectrum is produced from the ratio of the convolved weighted input values and the summed convolution function.

$$Spectrum(\nu) = Sum(\nu)/Weight(\nu) \quad (6)$$

3. Combination of Multiple Transitions

Both weak and strong lines may be averaged using this technique. Figure 6 shows the weighted average of HC_7N $J = 12-11$ and $J = 11-10$ transitions, along with the individual transitions offset by 0.5 K. Table 2 shows the measured intensities for the weighted average of the lines.

For molecules with simple structure, such as the cyanopolyynes, the line strength of closely spaced J rotational transitions changes smoothly and predictably. The line intensities are weak for larger interstellar molecules, and several days of observations are required to detect these transitions. For molecules with several closely spaced, similar strength, rotation transitions, the total observing time to required to obtain a desired signal to noise ratio is reduced linearly with the number of transitions observed. For weak molecular line detections, we have demonstrated (as expected) that the signal to noise ratio of the detection is doubled by averaging observations of four transitions. Larger linear molecules have many closely spaced, similar strength transitions, so no weighting for expected line strength is required.

We use the frequencies measured in the laboratory by McCarthy et al. (2000) to average observations of different ^{13}C isotopic species of HC_7N . Figure 7 shows intensity versus velocity plot for six HC_7N isotopomers observed daily. Figure 8 shows the intensity versus velocity plot for the system temperature and integration time weighted average. fit with a Gaussian model for the line intensity. The measured intensity of the HC_7N and isotopomers is given in Table 2.

To confirm the detection of the isotopomers, we performed a second observation towards TMC-HC₉N. Figure 9 shows the HC_7N $J = 12-11$ rotational transition for the observations of TMC-HC₉N. Figure 10 shows the weighted average of seven ^{13}C isotopomers of HC_7N

along with the individual lines, each offset by 0.1 K. Figure 11 shows the weighted average and a Gaussian fit to the average line. No significant emission was found at the frequency of DC_7N $J = 12 - 11$, with a 3σ upper limit of 0.019 K. No significant emission was found at the frequency of the ^{15}N isotopomer of HC_7N $J = 12 - 11$, with a 3σ upper limit of 0.019 K.

4. Comparison with Earlier Observations

Bell et al (1997) observed TMC-1 with the NRAO 140ft (43m) telescope and measured the brightness of the HC_7N $J = 12 - 11$ transition. For this transition, they found $T_B = 0.475 \pm 0.013$ K. This value is $\sim 50\%$ of the intensity measured with the GBT. At 13.5 GHz, the 140ft telescope FWHM beam width is $\sim 130''$. TMC-1 covers a smaller fraction of the 140ft telescope beam area. As figure 1 shows, TMC-1 is a roughly linear structure at the 140ft angular resolution, so we expect to measure a greater intensity with the GBT, roughly in relationship to the ratio of the GBT and 140ft telescope diameters.

Turner (2001) observed the DCN/HCN and $H^{13}CN/HCN$ abundance ratio for three interstellar clouds. For TMC-1, they use two radiative transfer models to estimate abundances. For their model "C" they found $DCN/HCN \sim 1/56$ and $H^{13}CN/HCN \sim 1/100$. These values are consistent with the average value we find for the isotopomers of HC_7N . Based on the observation of TMC-GB we find the abundance ratio $^{13}C/C$ is 1/87 with 1σ range 1/122 to 1/68. Based on the observation of TMC- HC_9N the abundance ratio $^{13}C/C$ is 1/132 with 1σ range 1/176 to 1/106. Averaging the measurements from the two positions yields abundance $^{13}C/C$ is 1/108 with 1σ range 1/136 to 1/90.

Takano et al. (1998) observed the ^{13}C isotopomers of HC_3N , and HC_5N in TMC-1. They find significant variation in the abundance ratios of the different isotopomers of HC_3N . For the TMC-1 they find $H^{13}CCCN/HC_3N = 79 \pm 11$, $HC^{13}CN/HC_3N = 75 \pm 10$, $HCC^{13}CN/HC_3N = 55 \pm 7$. Our average isotopic abundance is consistent with their results, but our observations do not have sufficient sensitivity to measure small differences in abundances of the different isotopic species.

For deuterium, our 3σ upper limit on the abundance ratio for DC_7N/HC_7N is 1/59. Turner (2001) has modeled the ^{13}C , deuterium and ^{15}N isotopomers of HCN and other IS molecules. For molecule HCN they find a DCN/HCN ratio range of 1/100 to 1/55, depending on the radiative transfer model assumed. This range is consistent with our limit.

Turner (2001) adopt abundance ratio of $HC^{15}N/HCN$ of 1/500. We find an upper limit for the abundance ratio of $HC_7^{15}N/HC_7N < 1/52$ (3σ).

It should be noted that for larger molecules, containing many atoms, the isotopic species are a significant fraction of the total molecular density. In the case of location TMC-GB, we find that the ^{13}C isotopomers of HC_7N are $7 \times 0.0099/0.864 \sim 8\%$ of the total molecular abundance.

5. Summary

We detect the ^{13}C isotopomers of HC_7N and place upper limits on DC_7N and HC_7^{15}N abundances.

We have demonstrated the benefits of averaging a number of weak rotational transitions of a molecule based on accurate laboratory measurement of spectral lines frequencies.

The GBT receiver, IF system and GBT spectrometer are great tools for observation of weak narrow molecular lines. The flexibility of the of configuring the four spectral bands is valuable for maximizing observing efficiency. However further expansion of the GBT IF and spectrometer are needed to fully observe all isotopic species of HC_7N in the GBT Ku-Band receiver frequency range. Currently we can simultaneously observe only 6 of the 42 transitions in this frequency range. A factor of 7 improvement in observing efficiency is possible for this project by expanding the spectrometer’s spectral coverage. Enhancing the spectrometers capabilities should be a priority for detecting the many weak rotational transitions expected for biologically significant molecules.

We thank P. Thaddeus, S. Breunken, C. Gottlieb, and M. McCarthy of the Harvard Center for Astrophysics for pointing out the possibility of detecting the HC_7N isotopomers. We thank Elizabeth Russell for help in organizing the data reduction effort. Thanks to R. Maddalena and T. Minter for helpful discussions on GBT calibration parameters. Thanks to F. Lovas for computing the HC_5N hyperfine transition frequencies. We thank the GBT operations and engineering staff for support during these observations. We acknowledge the very helpful suggestions of M. Hollis.

Facilities: NRAO

REFERENCES

- Bell, M. B., Feldman, P. A., Travers, M. J., McCarthy, M. C., Gottlieb, C. A., Thaddeus, P. (1997), ApJ, 483, 61

- Dickens, J.E., Langer, W. D. and Velusamy, T. 2001, *ApJ*, 558, 693.
- Dickey, John M. 2002, "In Single-Dish Radio Astronomy: Techniques and Applications", ASP Conference Proceedings, Edited by Stanimirovic, S., Altschuler, D., Goldsmith, P., and Salter, C., 278, 209.
- Hollis, J. M., Jewell, P. R., Lovas, F. J., Remijan, A. 2004, *ApJ*, 613, 45L.
- Kaifu, N. 2004, *PASJ*, 56, 69.
- Kalenskii, S. V., Slysh, V. I., Goldsmith, P. F. and Johansson, L. E. B. (2004), *ApJ*, 610, 329.
- Langston, G. I and Turner, B. 2007, *ApJ*, in preparation.
- Langston et al. 2007, *ApJ*, in preparation.
- McCarthy, M. C., Levine, E. S., Apponi, A., J., and Thaddeus, P. (2000), *Journal of Molecular Spectroscopy* 203, 75.
- Olano, C. A., Walmsley, C. M., Wilson, T. L. (1988), *A&A*, 196, 194.
- Pratap, P., Dickens, J. E., Snell, R. L., Miralles, M. P., Bergin, E. A., Irvine, W. M., Schloerb, F. P. (1997), *ApJ*, 486, 862.
- Ruze, R. 1966, *Proc. IEEE*, 54, No. 4, 633.
- Takano, Shuro et al., 1998 *A&A*, 329, 1156
- Turner, B. E. (2001), *ApJS*, 136, 579.
- Turner, B. E., Petrie, S., Dunbar, R. C., Langston, G. (2005), *ApJ*, 621, 817.

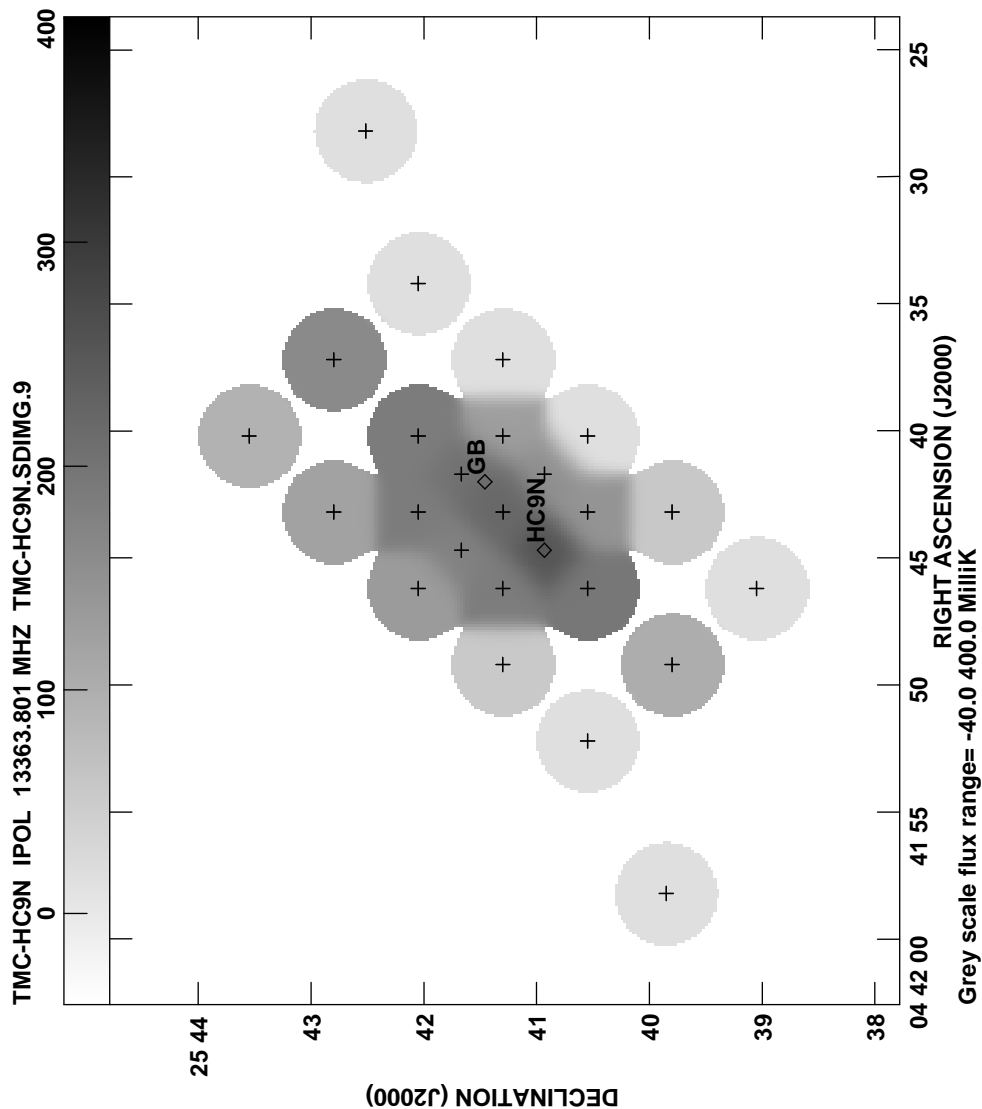


Fig. 1.— HC_9N molecular line intensity version position map of the TMC, from Langston and Turner (2007). The intensity scale is based on GBT observations of T_B calibrated average intensity of the HC_9N $J = 22 - 21$, $J = 23 - 22$, $J = 24 - 23$ and $J = 25 - 24$ rotational transitions. The location of the telescope pointings are shown with crosses. The image convolving function width is the $55''$. The locations of TMC-GB and TMC- HC_9N are marked with diamonds.

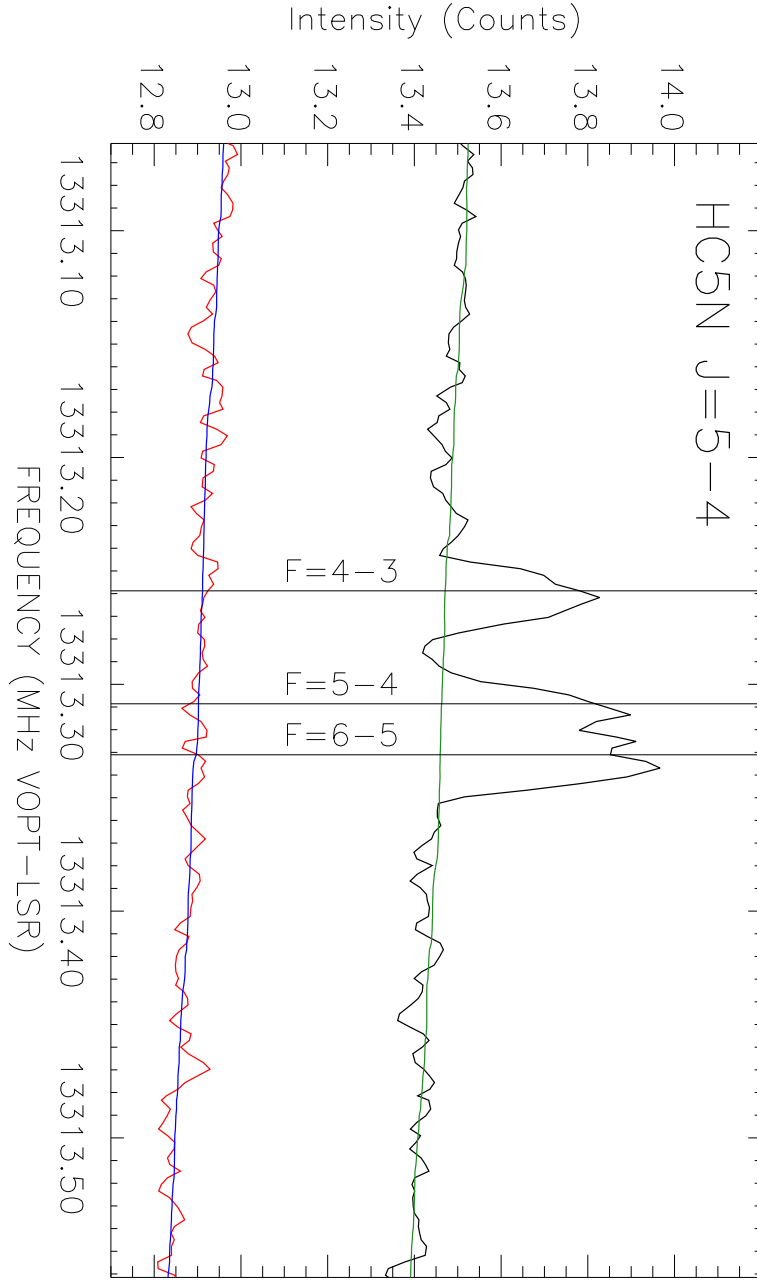


Fig. 2.— Intensity versus frequency plots centered on the three hyperfine transitions of the HC_5N $J = 5 - 4$ line. The upper spectrum (black) is the average of the signal beam observations, when pointed towards TMC-GB. The lower spectrum (red) is the average of the reference beam observations, which are offset $330''$ in azimuth from the signal beam location. Overlaid on the reference beam spectrum is the median filtered reference spectrum (blue), used for calibration of the signal spectrum. The median filter width is 0.5 MHz. For comparison, the median filtered signal spectrum (green) is also shown. For sufficiently wide filter window sizes, the molecular lines are completely removed.

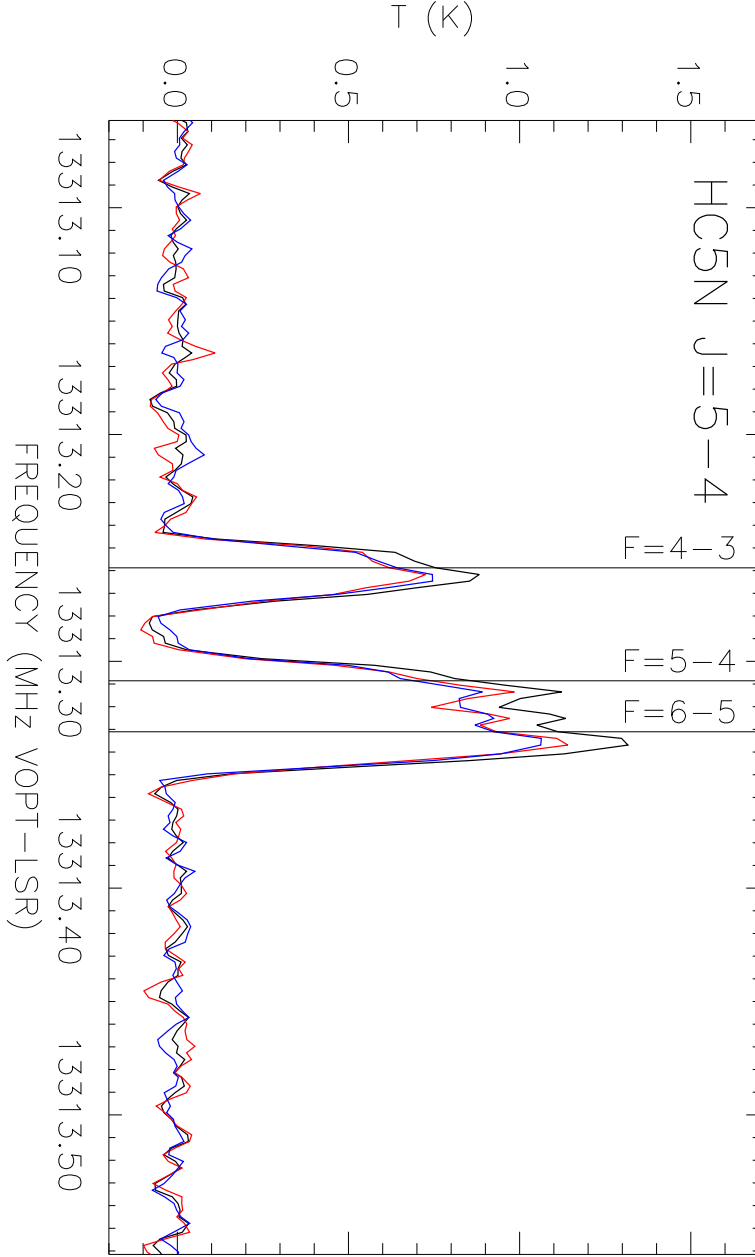


Fig. 3.— Three intensity versus frequency spectra, showing the fully T_B calibrated average spectrum (black) from a NOD observation of TMC-GB. The red spectrum is right circular polarization (RCP) and the blue spectrum is the left circular polarization (LCP). The RCP and LCP spectra are on the T_A scale, which does not include corrections for beam efficiency and atmospheric attenuation. A baseline has been subtracted from all three spectra, computed from a 0.5 MHz wide median filter of the original spectra. These spectra are from 3.8 minutes of observations on 2006 May 12. Three hyperfine transition frequencies are marked.

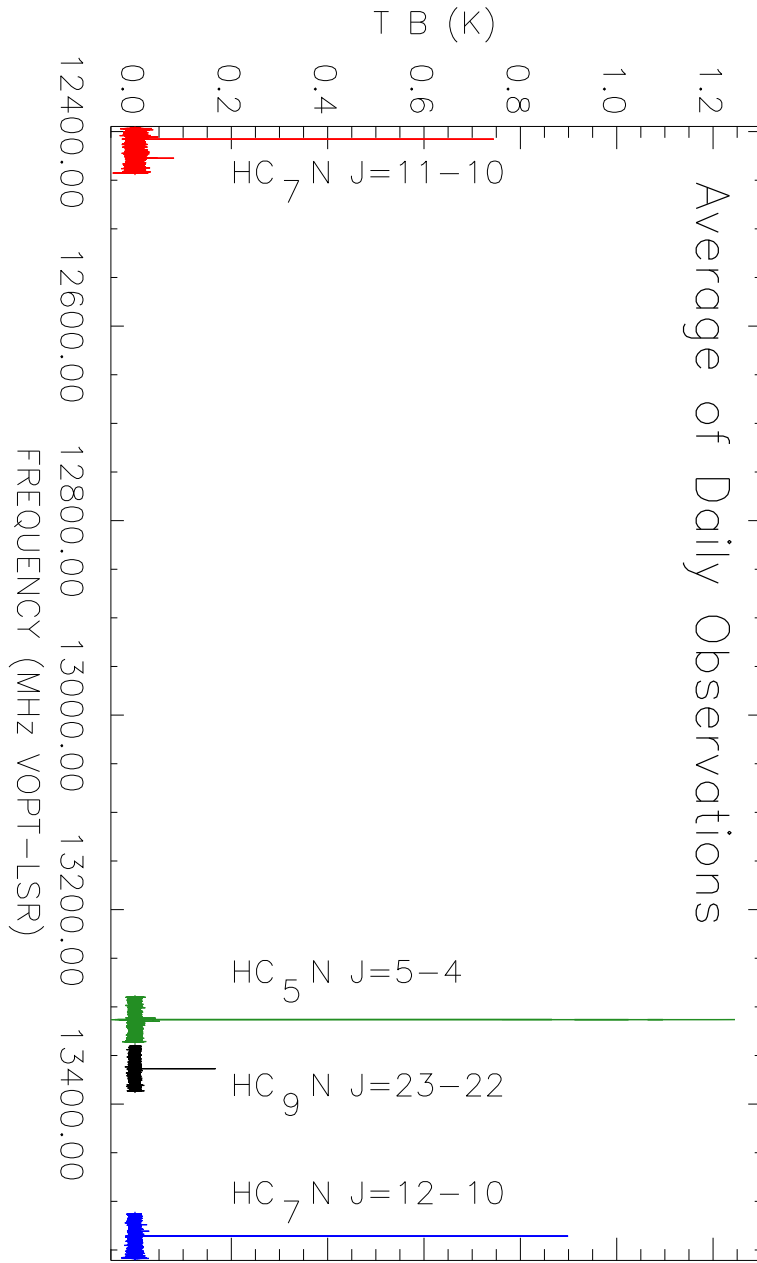


Fig. 4.— Intensity versus frequency plot showing daily system check observations for 11 to 15 GHz observations of TMC-GB, showing strong lines HC_5N $J = 5 - 4$ (green), HC_7N $J = 11 - 10$ (red), HC_7N $J = 12 - 11$ (blue) and HC_9N $J = 23 - 22$ (black). These spectra are produced from the average of 103 minutes of daily test observations in 2006.

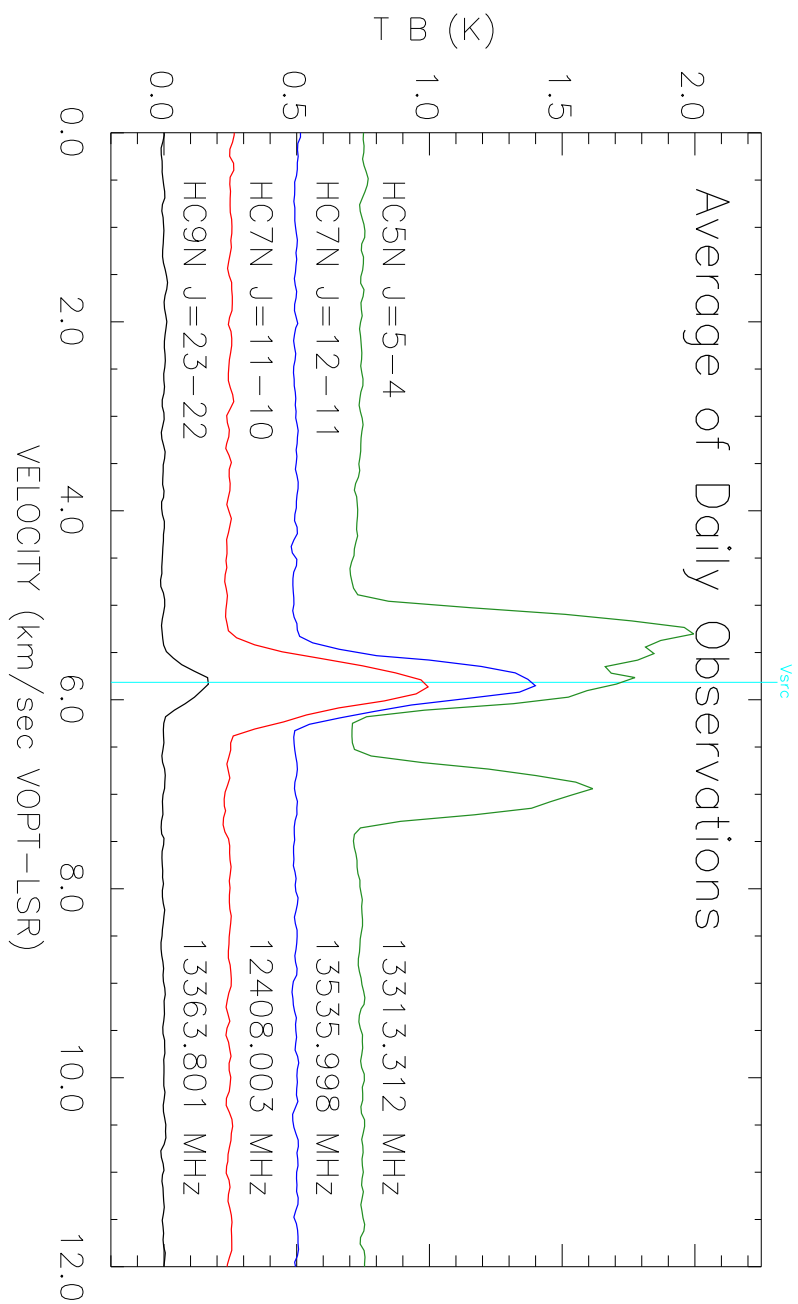


Fig. 5.— Intensity versus velocity plot for HC_9N , HC_7N and HC_5N lines detected in the daily system check observations. The lines are offset by 0.25 K for clarity. The plot shows the same data in the same colors as shown in the previous plot.

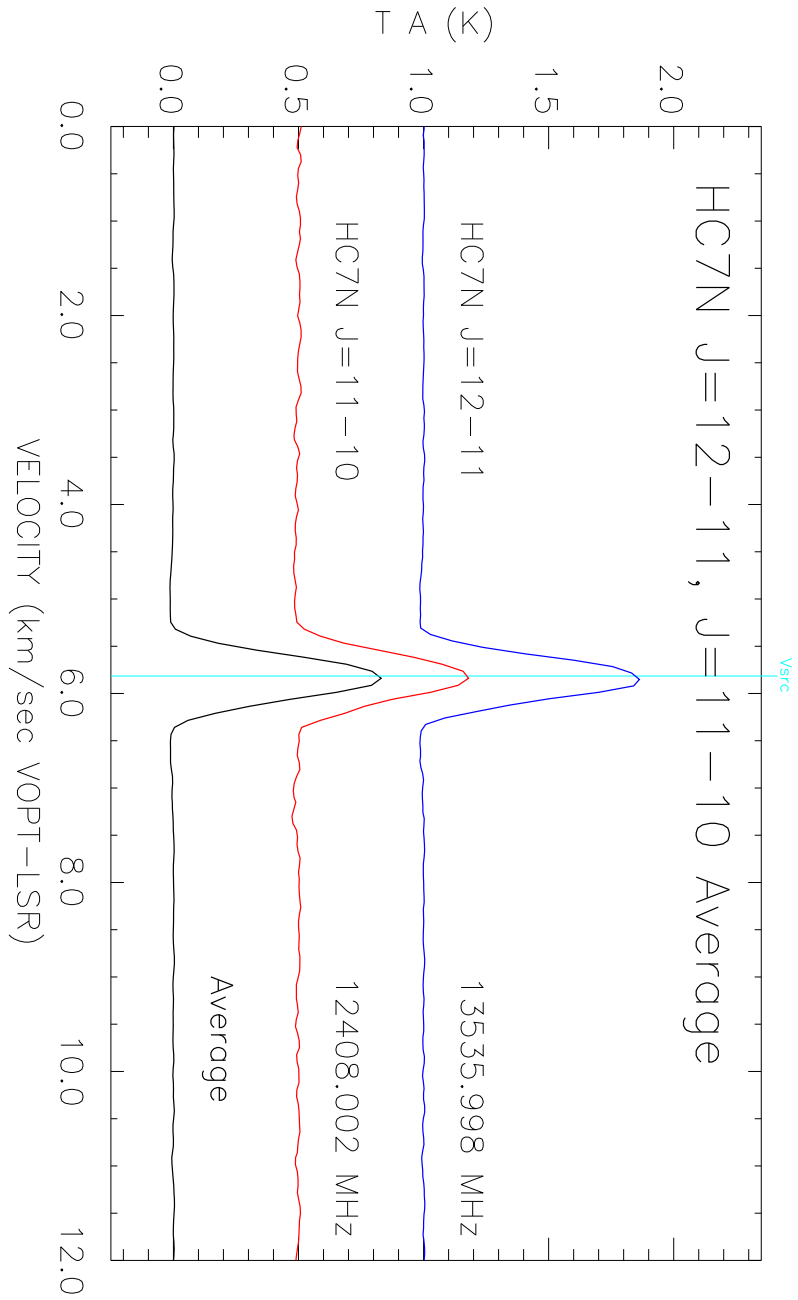


Fig. 6.— Intensity versus velocity plot for the average of the HC_7N $J = 12 - 11$ and $J = 11 - 10$ transitions at location TMC-GB. The weighted average of the two transitions is shown with zero offset. The two different $J' - J$ transitions are offset by 0.5 K. These spectra are produced from the average of 103 minutes of daily test observations in 2006.

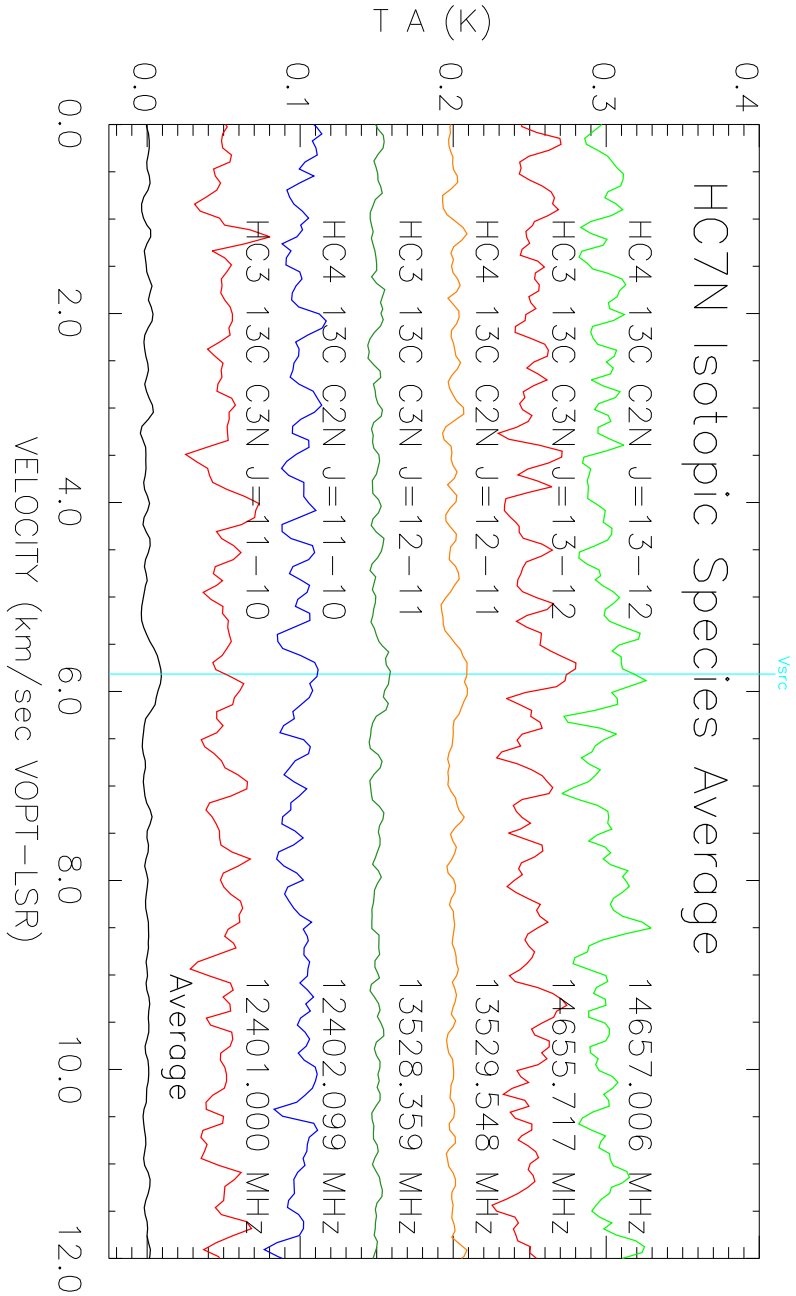


Fig. 7.— Intensity versus velocity plot for a weighted average of ^{13}C isotopic species of HC_7N listed in table 2. The weighted average is shown with no intensity offset and successive lines are shown with 0.1 K offsets. These spectra are produced from the average of 103 minutes of daily test observations in 2006.

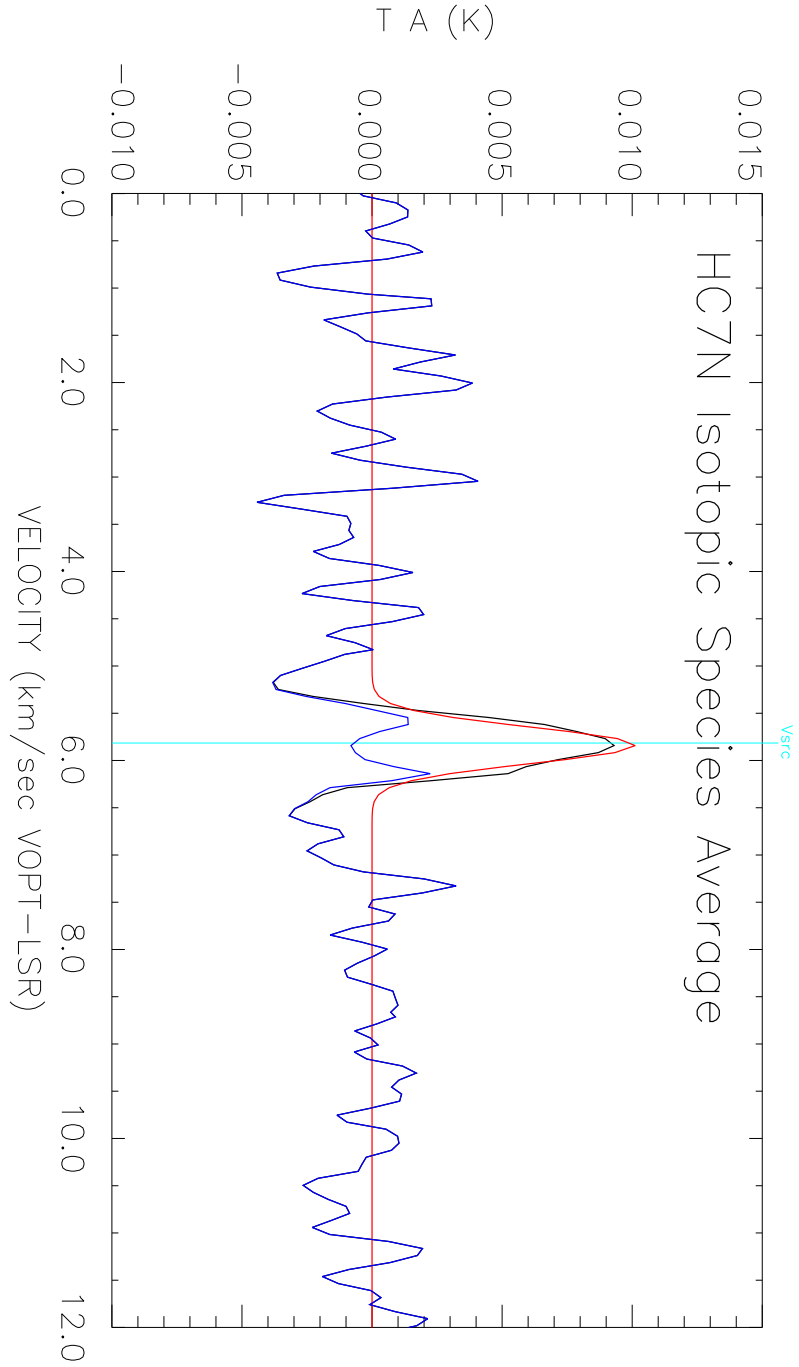


Fig. 8.— Intensity versus velocity plot for the weighted average of isotopomers of HC_7N . Same weighted average data as the previous plot. A single gaussian is fit to the average. The difference between fit and data is also shown. The vertical line shows the reference velocity 5.815 km/sec LSR.

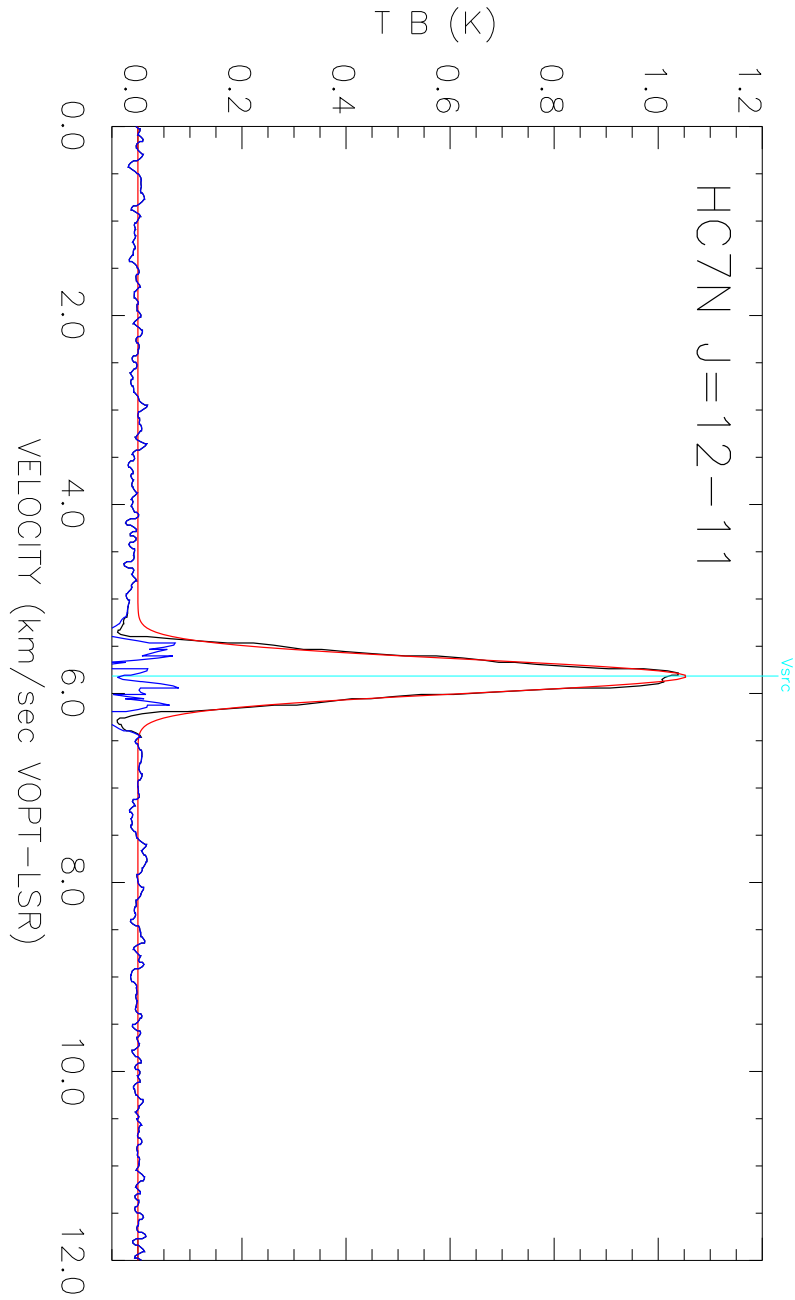


Fig. 9.— Intensity versus velocity plot for HC_7N $J = 12 - 11$ transition at location TMC- HC_9N . The smooth red line shows a Gaussian fit to the data. The difference between fit and data is also shown. Spectrum is produced from an average of 87.5 minutes of observations in September 2006.

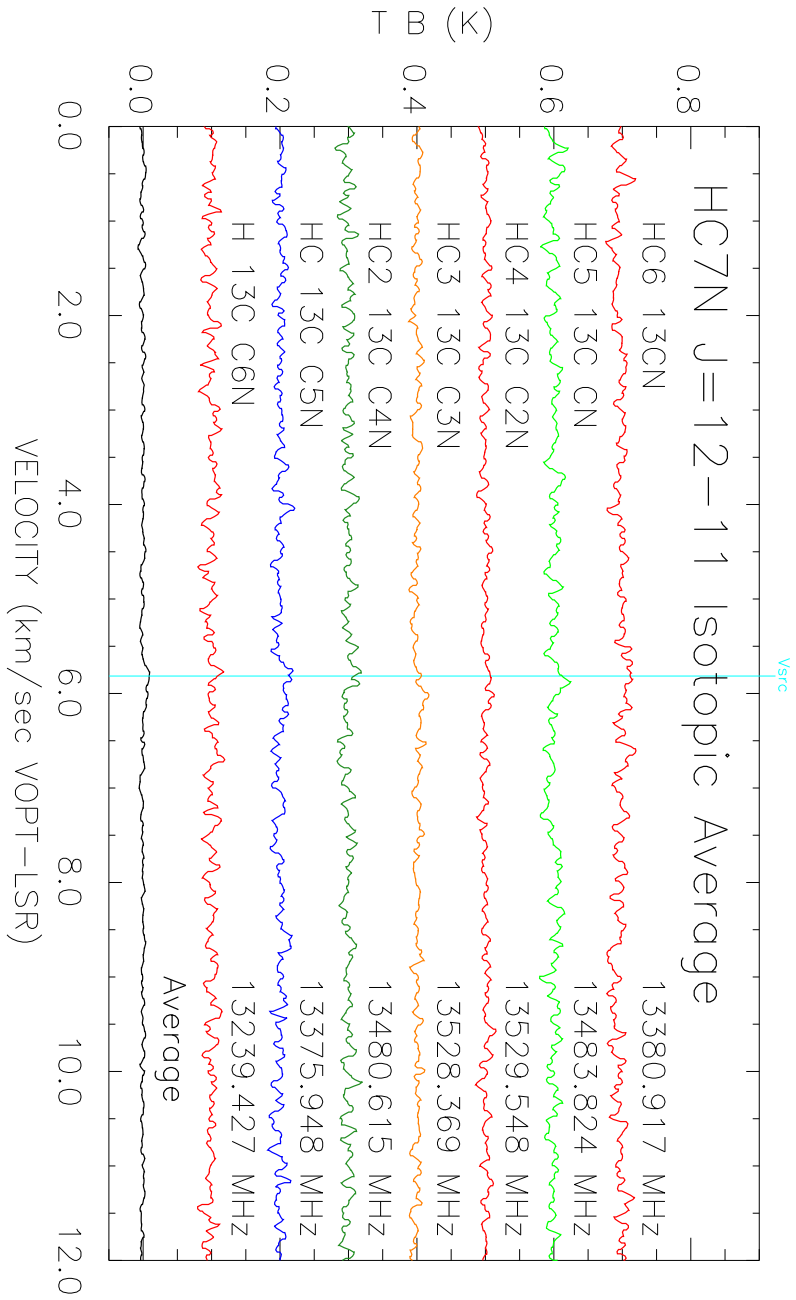


Fig. 10.— Intensity versus velocity plot for each of the ^{13}C isotopomers of HC_7N at the location TMC- HC_9N . The average of all lines listed in table 3 is shown with zero offset, and the isotopomers are shown with 0.1 K offsets. The vertical line show the reference velocity. Spectrum is produced from an average of observations in September 2006.

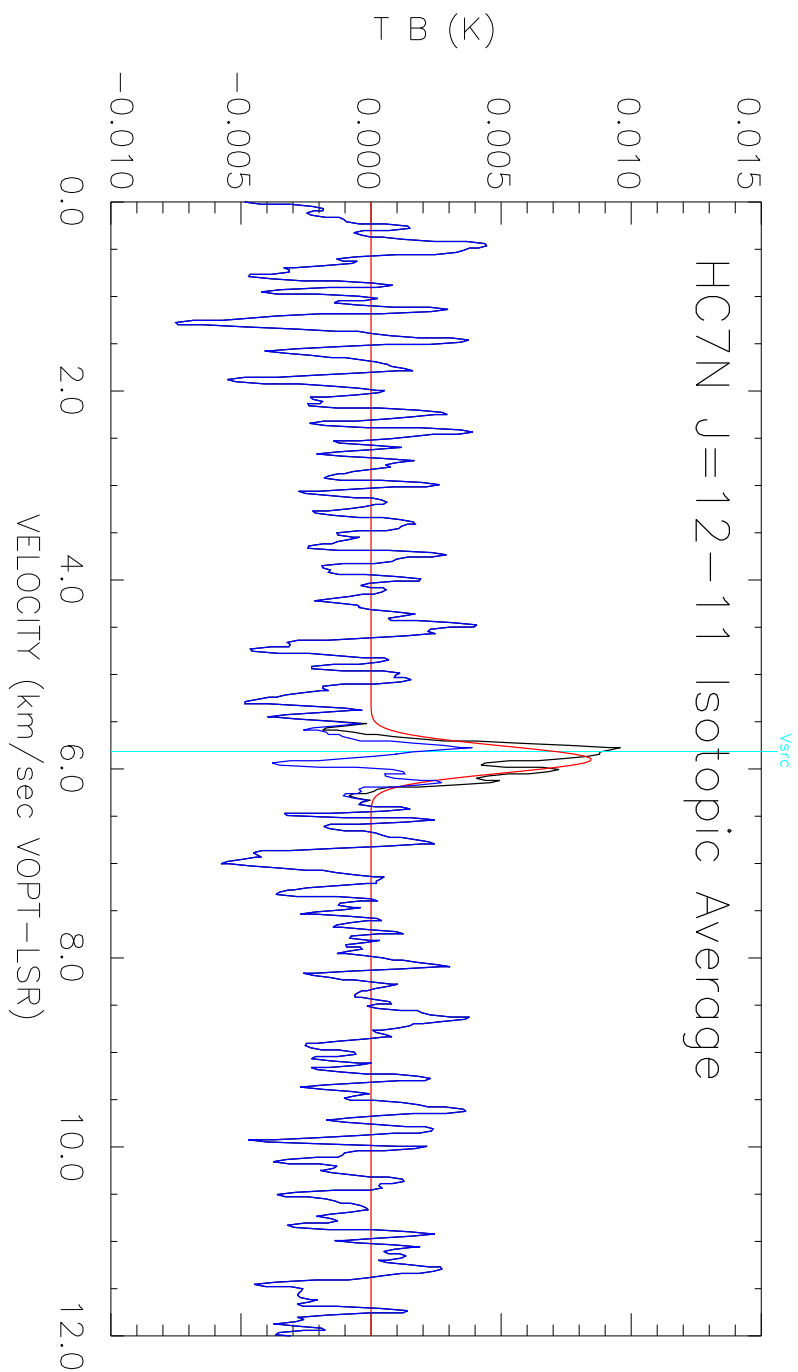


Fig. 11.— Intensity versus velocity plot for the average of the ^{13}C isotopomers of HC_7N at location TMC- HC_9N . Same weighted average data as the previous plot. The smooth red line shows a Gaussian fit to the data. The difference between fit and data is also shown.

Table 1: Cyanopolyynes Lines Observed Daily

Molecule	Transition		Rest Frequency (MHz)
	(J)	(F)	
<i>HC₅N</i>	5 – 4	4 – 3	13313.259
<i>HC₅N</i>	5 – 4	5 – 4	13313.309
<i>HC₅N</i>	5 – 4	6 – 5	13313.331
<i>HC₇N</i>	11 – 10		12408.003
<i>HC₇N</i>	12 – 11		13535.998
<i>HC₉N</i>	23 – 22		13363.801

Table 2: Observed lines of rotational transitions of isotopic species of HC_7N at location TMC-GB.

Molecule	Transition $J' - J$	Rest Frequency (MHz)	T_B (K)	v (km/s)	Δv FWHM (km/s)
HC_7N	11 – 10	12408.003	0.714 ± 0.007	5.825 ± 0.002	0.519 ± 0.003
HC_7N	12 – 11	13535.998	0.970 ± 0.005	5.819 ± 0.002	0.459 ± 0.003
HC_7N	average		0.864 ± 0.004	5.826 ± 0.004	0.492 ± 0.003
$HC_3^{13}CC_3N$	11 – 10	12401.000	< 0.023		
$HC_4^{13}CC_2N$	11 – 10	12402.093	< 0.023		
$HC^{13}CC_5N$	12 – 11	13375.947	< 0.014		
$HC_3^{13}CC_3N$	12 – 11	13528.359	< 0.017		
$HC_4^{13}CC_2N$	12 – 11	13529.548	< 0.017		
$HC_6^{13}CN$	12 – 11	13380.917	< 0.015		
^{13}C Isotopic Ave	12 – 11		0.0099 ± 0.003	5.782 ± 0.054	0.52 ± 0.13

Table 3: Observed lines of rotational transitions of isotopic species of HC_7N at location TMC-HC₉N.

Molecule	Transition $J' - J$	Rest Frequency (MHz)	T_B (K)	v (km/s)	Δv FWHM (km/s)
HC_7N	12 – 11	13535.998	1.101 ± 0.007	5.815 ± 0.001	0.426 ± 0.001
DC_7N	12 – 11	13087.538	< 0.019		
$HC_7^{15}N$	12 – 11	13254.054	< 0.019		
$H^{13}CC_6N$	12 – 11	13239.427	< 0.019		
$HC^{13}CC_5N$	12 – 11	13375.947	< 0.019		
$HC_2^{13}CC_4N$	12 – 11	13480.615	< 0.019		
$HC_3^{13}CC_3N$	12 – 11	13528.359	< 0.015		
$HC_4^{13}CC_2N$	12 – 11	13529.548	< 0.015		
$HC_5^{13}CCN$	12 – 11	13484.825	< 0.019		
$HC_6^{13}CN$	12 – 11	13380.917	< 0.019		
^{13}C Isotopic Ave	12 – 11		0.0084 ± 0.0022	5.902 ± 0.013	0.348 ± 0.030